Overcoming the solid solubility limit of Te in Ge by ion implantation and pulsed laser melting recrystallization.

D. Caudevilla[1,*], Y. Berencén[2], S. Algaidy[1], F. Zenteno[1], J. Olea[1], E. San Andrés[1], R. García-Hernansanz[1], A. del Prado[1], D. Pastor[1], E. García-Hemme[1]

[1]Dpto. EMFTEL, Fac. CC. Físicas, Univ. Complutense de Madrid, 28040 Madrid, Spain; *danicaud@ucm.es
[2]Helmholtz-Zentrum Dresden-Rossendorf, Institute of Ion Beam Physics and Materials Research, Bautzner Landstr. 400, 01328 Dresden, Germany.

Abstract—**Germanium hyperdoped with deep level donors, such as tellurium, would lead to dopant-mediated sub-band gap mid-infrared photoresponse at room temperature. We use a combination of non-equilibrium techniques to supersaturate Ge with Te via ion implantation followed by pulsed laser melting (PLM). Typically, liquid N_2 (77K) temperatures are used to avoid implantation-induced Ge surface porosity. In this work, alternatively, we report on the use of slightly higher implantation temperatures (143 K) together with an amorphous Si (a-Si) capping layer. We demonstrate that the solid solubility limit of Te in Ge is overcome upon recovering the crystallinity of the material after laser processing.**

Keywords— ion implantation, PLM, germanium, tellurium, capping layer.

I. Introduction

Short and mid-infrared (SWIR and MWIR) sensing based on CMOS compatible semiconductors is a technological challenge, and it has many applications, such us surveillance, security and sensing [1]. Germanium hyperdoped with deep level donors, such as tellurium, would lead to extrinsic dopant-mediated sub-bandgap absorption at room temperature [2, 3]. In this work, we report on the use of two non-equilibrium techniques to supersaturate germanium with tellurium: ion implantation followed by pulsed laser melting (PLM).

Ion implantation in germanium with heavy ions, at high dose or at high energies produces porosity in the substrate surface which makes it impossible to recover the crystallinity of the material after any annealing process [4, 5]. To avoid this implantation-induced Ge surface damage, LN_2 (77 K) temperatures are typically used [6]. In this work, we propose to use alternatively slightly higher implantation temperatures (143 K) together with an a-Si capping layer [7].

We implanted with doses several orders of magnitude above the solid solubility limit of Te in Ge and analyse the structural properties of the implanted layers before and after laser processing by Raman, Time of Flight Secondary Ion Mass Spectroscopy (ToF-SIMS) and Transmission Electron Microscopy (TEM).

II. EXPERIMENTAL

DSP, 300 µm <100> p-Ge wafers (1 Ω·cm) provided by Umicore were implanted with $^{130}Te^+$ at doses of 10^{14} cm^{-2} and 10^{16} cm^{-2} with an energy of 120 keV. To mitigate the surface implantation-induced damage produced by heavy ions at high energy, a 50-nm-thick a-Si capping layer was sputtered on top of the wafers prior to the implantation. This protective layer is combined with ion implantation temperatures below 143 K during the whole process.

After ion implantation, the wafers were cut in 5×5 mm^2 square samples. The a-Si capping layer was selectively removed without etching the Ge substrate by submerging the samples in a Tetramethylammonium hydroxide (TMAH) solution (25%) at 60 ºC during 5 min. After the etching process, the samples were pulsed-laser melted with a XeCl (308 nm) excimer laser (Coherent COMPexPRO201), with a pulse duration of 28 ns and an energy density of 0.5 J·cm^{-2}. All the fabrication steps were performed at Helmholtz-Zentrum Dresden-Rossendorf's facilities.

The in-depth profiles of the Te implanted samples were obtained by ToF-SIMS at C.A.C.T.I. of University of Vigo with Bi^{3+} used as a primary ion at 25 kV.

The phonon spectra were determined by µ-Raman spectroscopy in the wavenumber range of 100-550 cm^{-1} using the line 532 nm of a Nd:YaG laser as exciting source. This technique allows us to analyse the crystal quality of the implanted layers and to detect other elements incorporation in the Ge lattice, such as Si coming from the capping layer.

TEM images were obtained with a JEOL JEM 2100 using an acceleration energy of 200 kV to analyze the crystal structure, whereas Energy Dispersive X-Rays Spectroscopy (EDS) was used to characterize the material composition. The lamellas for TEM were prepared by Focused Ion Beam (FIB) with a Helios Nanolab 650 system at University of Zaragoza and measured at CNME (UCM).

III. RESULTS

The tellurium concentrations in-depth profiles are shown in Fig. 1. In the Te as-implanted samples, the 72% of the implanted Te atoms were found to penetrate the Ge substrate, while a 28% of the implanted atoms remained in the capping layer. Those values are the same for both doses. After removing the a-Si layer and performing the PLM process, Te was found to be redistributed deeper into the substrate. Nevertheless, even for the lowest dose and after PLM, we observe that the Te solid solubility limit in Ge (2×10^{15} cm^{-3}, Ref. [8]) is surpassed by three orders of magnitude in the first 50 nm layer.

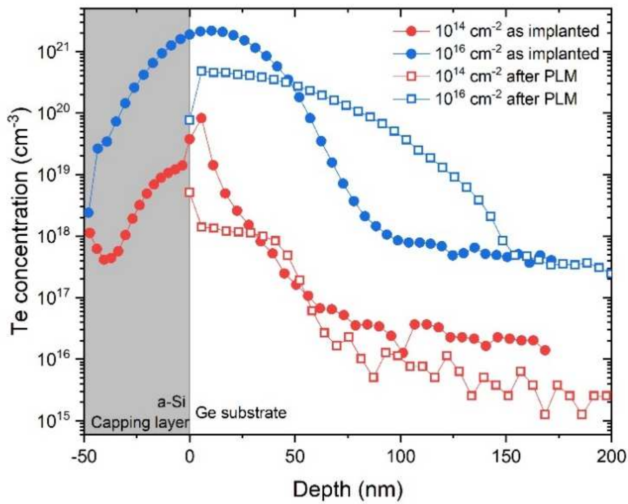

Fig. 1. ToF-SIMS profiles of low- (10^{14} cm^{-2}) and high-dose (10^{16} cm^{-2}) implanted Ge:Te before (filled circles) and after PLM (open squares). The first 50 nm corresponds to the a-Si capping layer.

Fig. 2 shows the Raman spectra of the implanted samples before PLM (after the a-Si capping layer etching), and after the PLM process. Even for the lowest implanted dose, the Ge substrate is amorphized due to the ion implantation. For the lowest dose we detect the crystalline peak of the Ge substrate because the penetration depth of the 532-nm laser excitation is greater than the thickness of the amorphous layer. After PLM, however, the samples of both doses show a great recovery of the crystallinity.

For the highest dose, the c-Ge vibrational mode shows a low-frequency asymmetry, which is related to a partial lack of crystallinity. The down-shift of the Ge-Ge peak at 300 cm-1 likely originates from strain, induced by the Te incorporation. Note that after the PLM process of the highest dose sample, a peak at 380 cm^{-1} appears in the Raman spectra, which corresponds to the Si-Ge bonding after PLM process. However, there is no sign of the amorphous Si band which would correspond to the a-Si capping layer before PLM for any of the samples, indicating that it has been successfully removed.

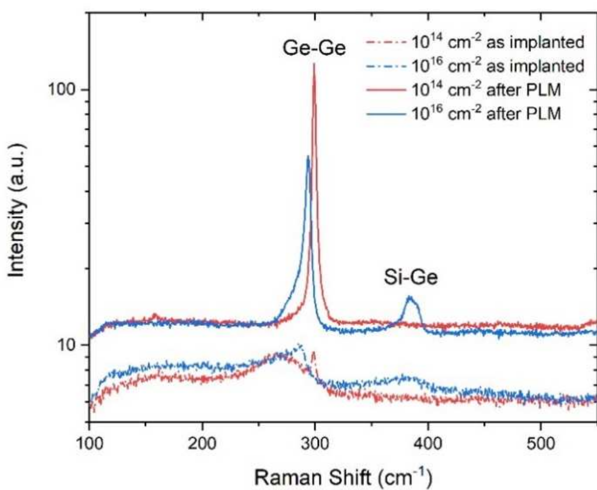

Fig. 2. Raman spectra of Te-implanted Ge samples at different doses (10^{14} cm^{-2} in red and 10^{16} cm^{-2} in blue). The dashed lines correspond to the samples before PLM and the filled lines to PLM processed samples with a fluence of 0.5 $J{\cdot}cm^{-2}$. We indicate the peaks corresponding to Ge-Ge bonding (at 300 cm^{-1}) and to Ge-Si bonding (at 380 cm^{-1}).

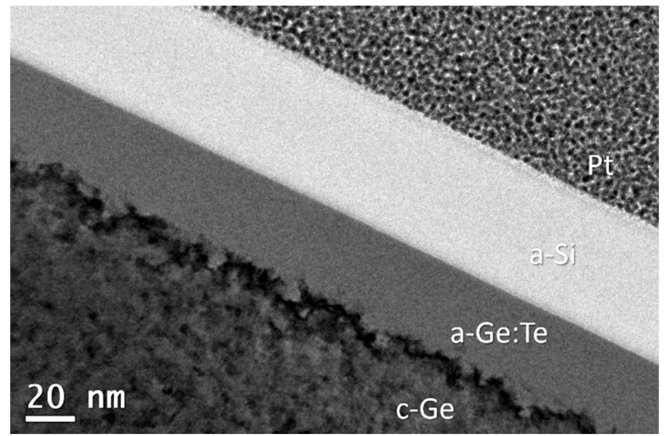

Fig. 3. TEM image of a germanium substrate as implanted with Te^{+} at a dose of 10^{14} cm^{-2}. From top-right to bottom-left we see the Pt from sample preparation, the a-Si capping layer, and the germanium substrate, amorphized in the first 40 nm.

The Si-Si bands, which could appear around 150 cm^{-1} and 470 cm^{-1} are not present in the spectra. We analysed them to optimize the a-Si etching. The Si-Ge peak indicates that there is Si bonding to Ge into the substrate introduced during ion implantation, as measured by ToF-SIMS (not shown).

Fig. 3 and 4 show the TEM images from the two as-implanted samples with the capping layer. On the one hand, for the lowest dose (Fig. 3), the interface between the a-Si capping layer and the amorphized Ge substrate is perfectly defined. The thickness of the a-Si capping layer is 50 nm and the thickness of the amorphized Ge is around 40 nm. Those values are in accordance with the simulated profiles by Stopping and Range of Ions in Matter (SRIM) software (not shown). On the other hand, for the highest dose (Fig. 4) the amorphous region is 150 nm thick. In this region the a-Si capping layer is intermixed with the Ge substrate amorphized by ion implantation. This layer intermixing has also been observed by EDS.

After the a-Si capping layer etching and the PLM process, we observe in Fig. 5 and 6 that the crystallinity of the implanted layer is fully recovered, with no signs of extended defects or inhomogeneous distribution of Te. There is no sign of the a-Si capping layer and the selected-area electron diffraction (SAED) diagram (the inset in both figures) corroborates the good crystallinity.

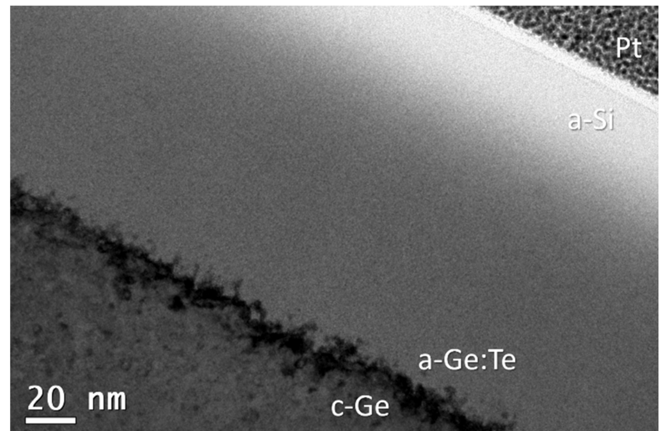

Fig. 4. TEM image of a germanium substrate as implanted with Te^{+} at a dose of 10^{16} cm^{-2}. From top-right we see the Pt from sample preparation and then the a-Si capping layer mixed with the amorphized Ge substrate (150 nm in total).

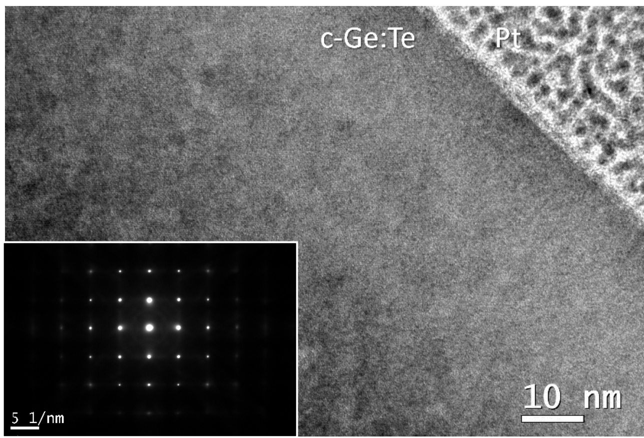

Fig. 5. TEM image of the recrystallized Ge:Te implanted at a dose of 10^{14} cm^{-2}. The a-Si was removed before PLM. In the inset we can see the SAED diagram to verify the crystallinity.

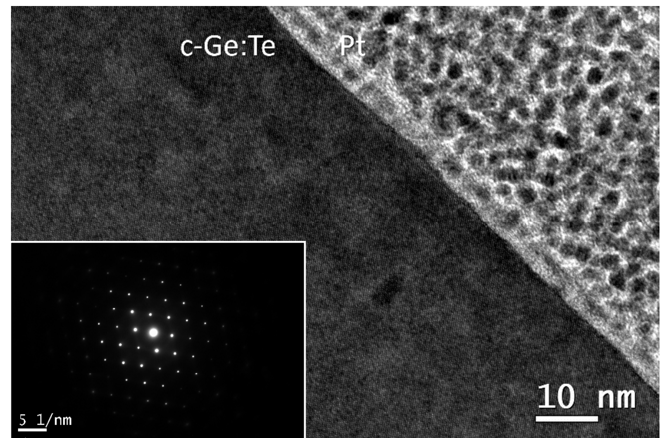

Fig. 6. TEM image of the recrystallized Ge:Te implanted at a dose of 10^{16} cm^{-2}. The a-Si was removed before PLM. In the inset we can see the SAED diagram to verify the crystallinity.

Furthermore, EDS confirms Te incorporation above 5% into the Ge layer at the highest dose, before and after laser melting, which is in accordance with the ToF-SIMS results. The detection limit of this technique is around 1%, so it is not possible to compare for the lowest dose sample.

IV. CONCLUSIONS

In this work, we have demonstrated that Ge layers can be supersaturated with Te concentrations several orders of magnitude above its solid solubility limit with non-equilibrium techniques, such as ion implantation and PLM. The resulting supersaturated Ge:Te layers are fully recrystallized without extended defects or Te inhomogeneity distribution after the PLM process. We also demonstrate that the use of an a-Si capping layer together ion implantation at 143 K, which is several tens above the LN_2 temperature, can be used to supress the Ge surface porosity during the ion implantation.

These promising results would lead to the fabrication of optoelectronic devices for sensing in the SWIR and MWIR range. Future works with these samples will involve electrical and optoelectronic measurements to analyse the electrical activation and the sub-bandgap spectral photoresponse at room temperature.

ACKNOWLEDGMENTS

The authors acknowledge the ToF-SIMS measurements driven by Servicio de Nanotecnología y Análisis de Superficies at CACTI (Universidad de Vigo). Authors acknowledge the use of instrumentation as well as the technical advice provided by the National Facility ELECMI ICTS, node "Laboratorio de Microscopías Avanzadas" at University of Zaragoza and TEM images at CNME (Universidad Complutense de Madrid).

This work is part of the project TEC2017-84378-R, funded by MICINN and European Social Fund and project MADRID-PV2 (P2018/EMT-4308) funded by the Comunidad Autónoma de Madrid with the support from FEDER Funds. Parts of this research were carried out at IBC at the Helmholtz–Zentrum Dresden–Rossendorf e. V., a member of the Helmholtz Association. Authors would like to thank Ulrich Kentsch for his assistance with the low-temperature implantations. D. Caudevilla would also acknowledge grant PRE2018-083798, financed by MICINN and European Social Fund. D. Pastor acknowledges financial support from the program Ramón y Cajal (Grant No. RYC-2014-16936).

REFERENCES

[1] Rogalski, A. (2011). Recent progress in infrared detector technologies. Infrared Physics & Technology, 54(3), 136-154.

[2] Gandhi, H. H., Pastor, D., Tran, T. T., Kalchmair, S., Smilie, L. A., Mailoa, J. P., ... & Mazur, E. (2020). Gold-Hyperdoped Germanium with Room-Temperature Sub-Band-Gap Optoelectronic Response. Physical Review Applied, 14(6), 064051.

[3] Gandhi, H. H., Pastor, D., Tran, T. T., Kalchmair, S., Smillie, L. A., Mailoa, J. P., ... & Mazur, E. (2020). Chalcogen-hyperdoped germanium for short-wavelength infrared photodetection. AIP Advances, 10(7), 075028.

[4] Stepanov, A. L., Nuzhdin, V. I., Valeev, V. F., Rogov, A. M., Vorobev, V. V., & Osin, Y. N. (2018). Porous germanium formed by low energy high dose Ag+-ion implantation. Vacuum, 152, 200-204.

[5] Impellizzeri, G., Romano, L., Bosco, L., Spinella, C., & Grimaldi, M. G. (2012). Nanoporosity induced by ion implantation in germanium thin films grown by molecular beam epitaxy. Applied Physics Express, 5(3), 035201.

[6] Impellizzeri, G., Mirabella, S., & Grimaldi, M. G. (2011). Ion implantation damage and crystalline-amorphous transition in Ge. Applied Physics A, 103(2), 323-328.

[7] Tran, T. T., Alkhaldi, H. S., Gandhi, H. H., Pastor, D., Huston, L. Q., Wong-Leung, J., ... & Williams, J. S. (2016). Suppression of ion-implantation induced porosity in germanium by a silicon dioxide capping layer. Applied Physics Letters, 109(8), 082106.

[8] Abrikosov, N. K. (2013). Semiconducting II–VI, IV–VI, and V–VI Compounds. Springer